

Death by Dynamics: Planetoid-Induced Explosions on White Dwarfs

Rosanne Di Stefano

Harvard-Smithsonian Center for Astrophysics

Robert Fisher

University of Massachusetts Dartmouth

James Guillochon

Harvard University

James F. Steiner

Harvard-Smithsonian Center for Astrophysics

Received _____; accepted _____

ABSTRACT

At intervals as short as ten thousand years, each white dwarf (WD) passes within a solar radius of a planetoid, i.e., a comet, asteroid, or planet. Gravitational tidal forces tear the planetoid apart; its metal-rich debris falls onto the WD, enriching the atmosphere. A third of WDs exhibit atmospheric “pollution”. For roughly every hundred planetoid disruptions, a planetoid collides with a WD. We simulate a small number of collisions, in which “death-by-dynamics” refers to the fate of the planetoid. We also compute the energies and likely durations of a broad sample of collision events, and identify detection strategies at optical and X-ray wavelengths. Collisions with the most massive planetoids can be detected in external galaxies. Some may trigger nuclear burning. If one in $\sim 10^7 - 10^8$ of WD-planetoid collisions creates the conditions needed for a Type Ia supernova (SN Ia), “death-by-dynamics” would also refer to the fate of the WD, and could provide a novel channel for the production of SN Ia. We consider the circumstances under which the rate of SNe Ia can be increased by interactions with planetoids.

1. Planetoids, Collisions with White Dwarfs, and the Generation of Type Ia Supernovae

1.1. White Dwarfs and Tidal Disruptions

Planets around white dwarfs (WDs) have yet to be discovered, but several lines of reasoning suggest that WDs commonly host planetary systems (Di Stefano 2011; Parriott & Alcock 1998). The strongest evidence is that more than 1/3 of WDs exhibit substantial atmospheric “pollution”. The mechanism responsible appears to be the tidal disruption

(TD) of planetoids (Jura 2008; Zuckerman et al. 2010; Farihi et al. 2013).

Because the metal settling time can be $\sim 10^5$ years (Koester 2009), contributions from planetoids can be assessed only in aggregate. The average mass influx is estimated to be $\dot{M} = (10^{15} - 10^{17})$ g/yr (Zuckerman et al. 2010; Barber et al. 2012). Some WDs may therefore accrete up to an Earth mass of metal-rich material during a Hubble time.

The mass is deposited by sequences of incident planetoids: comets, asteroids, and planets. To relate \dot{M} to the influx of planetoids, we use a power-law mass distribution, $\frac{dN(M)}{dM} \propto M^{-\beta}$, with $\beta = 1.75$. Here, $dN(M)$ is the number of objects with mass between M and $M + dM$. Thus, the measured rate of pollution can be provided by the disruption of one 10^{12} g TD per year, one 10^{15} g TD per century, or one 10^{21} g TD per Myr. The mass distribution predicts a mix of masses and time intervals between events.

1.2. Collisions

If planetoids come close enough to WDs for TDs, then some must collide with WDs. Because the cross section for close approaches is proportional to the distance of closest approach, the collision rate is $\sim 1\%$ the rate of TDs, scaling roughly as the ratio R_{WD}/R_{\odot} , where R_{WD} is the radius of the WD, and R_{\odot} is very close to the tidal radius at which disruption occurs (e.g., Pineault & Landry 1994; Schlichting et al. 2013; Fuentes et al. 2010). The word “death” in our title can therefore refer to the certain destruction of a planetoid when it collides with a WD. In §2 we show the results of a small number of simulated collisions and then compute the detectable effects of a larger number across the mass range spanning from comets to planets.

1.3. Type Ia Supernovae

In extreme cases, a sequence of TDs and collisions may spark nuclear burning, potentially providing a novel pathway to SNe Ia. If interactions with planetoids can help propel WDs to SN Ia explosions, the word “death” in our title may also refer to the end of the WD. The addition of a new evolutionary pathway may be a positive step toward developing a better understanding of how SNe Ia are generated. Observations tell us that of every fifty WDs, one ends as a Type Ia supernova (SN Ia). Yet calculations based on the standard models have difficulty producing rates this high (Nelemans et al. 2013).

2. Collisions between WDs and Planetoids

2.1. Energy of WD-Planetoid Collisions

An incoming planetoid is subject to strong tidal forces once it crosses its tidal radius $r_t = R_{\text{WD}}(\bar{\rho}_{\text{WD}}/\bar{\rho}_{\text{pl}})^{1/3}$, where $\bar{\rho}_{\text{WD}}$, $\bar{\rho}_{\text{pl}}$ are the average densities of the WD and planetoid, respectively. At this moment, the planetoid disintegrates (likely into chunks) and has a spread in binding energies $\Delta E = GM_{\text{WD}}R_{\text{WD}}/r_t^2$ that translates to a spread in times of impact $\Delta t \simeq (R_{\text{pl}}/r_t)t_{\text{ff}}$, where t_{ff} is the amount of time elapsed between when the planetoid crosses r_t ($\simeq 0.5 R_{\odot}$ for $M_{\text{WD}} = M_{\odot}$) and when it impacts the WD’s surface, $t_{\text{ff}} = \pi\sqrt{r_t^3/8GM_{\text{WD}}} \sim 10$ min. For a 4 km planetoid with $\bar{\rho}_{\text{pl}} = 10$ g cm³ this spread would only be 7 ms, corresponding to an impactor whose length has increased by a factor of ~ 5 .

This modest increase in length means that the impactor strikes the surface of the WD in a small area, comparable to its own size, rather than being spread over the WD’s surface à la the Shoemaker-Levy comet which impacted Jupiter on its second periape (Asphaug & Benz 1996). We simulate a two examples of planetoid impacts using the hydrodynamical code FLASH (Fryxell et al. 2000), the results of which are presented in Figure 1. We find

that the planetoid penetrates to a depth where the density of the WD’s atmosphere is a factor of ~ 10 greater than $\bar{\rho}_{\text{pl}}$, with the surface and the impactor being heated to a few million degrees. After impact, the ejecta quickly expands and cools, initially radiating in the X-rays for \sim tens of milliseconds for the 4 km impactor, longer for more massive impactors, but releasing the majority of its energy in the optical over longer timescales.

2.2. Event Detection

State-of-the art optical surveys – e.g., Pan-STARRS (Kaiser et al. 2002), Palomar Transient Factory (PTF; Rau et al. 2009), SkyMapper (Keller et al. 2007), GAIA (Perryman et al. 2001), Palomar-Quest (Djorgovski et al. 2008), Catalina Real-Time Transient Survey (Drake et al. 2009) – can reach a field depth up to roughly ~ 21 mag per observation (in one-to-several minutes exposure time; Rau et al. 2009, and references therein). We adopt the combined characteristics of Pan-STARRS and PTF as our benchmark. Current surveys yield sky coverage up to several thousands of square degrees each night. To classify a collision event as robustly detectable by present surveys, we adopt a strong threshold of 20 mag, in order that non-detections in data bracketing the transient event can be discriminating. To estimate an event’s detectability, we adopt a time of 100 s for a ground-based exposure and neglect interstellar extinction. We assume 100% efficiency in the conversion of gravitational potential energy into optical radiation (for simplicity, we neglect any bolometric correction). The emission timescale is calculated following Arnett’s law (Arnett 1980) for an expanding gas. Recombination is the dominant source of emission, and continues until the gas has fully recombined, a timeframe which scales linearly with the size of the impactor, with a rule of thumb ~ 1 s/km. The *effective* optical luminosity \tilde{L}_{opt} is the luminosity an observer would infer from a 100s exposure around the peak. Note that when the emission timescale becomes very short, the effective luminosity will be lower than

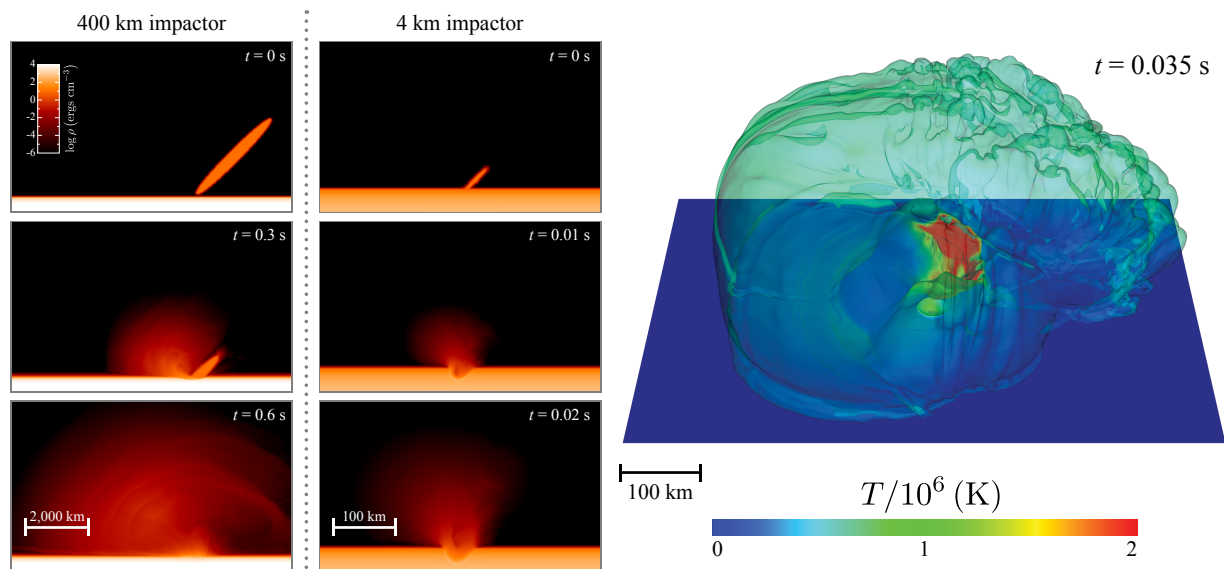


Fig. 1.— Results from two hydrodynamical simulations of the impact of a tidally stretched bolide with a WD atmosphere. The left three panels show 2D slices of $\log \rho$ as a function of time t through the plane of symmetry for an impactor initially 400 km in radius, where the impactor travels right to left at a 45° angle to the WD’s surface. The middle three panels show the same for a 4 km impactor. The right panel shows a 3D snapshot from the 4 km impactor simulation, with the contour corresponding to the region that contains at least 10% of the impactor’s composition by mass, color-coded by temperature.

the short-lived peak luminosity.

While optical surveys cover regions of the sky at a specified cadence, X-ray monitors (e.g., Swift BAT, Barthelmy et al. 2005; RXTE ASM, Levine et al. 1996; MAXI GSC, Mihara et al. 2011; Integral IBIS, Ubertini et al. 2003), often cover nearly the full sky continuously, producing \sim daily maps of the brightest X-ray sources. One of the most-sensitive of these monitors, the MAXI GSC, can detect source fluences of ~ 50 Crab seconds per orbit (i.e., $\approx 10^{-6}$ erg cm $^{-2}$, corresponding a persistent X-ray flux $\lesssim 50$ mCrab $\approx 10^{-9}$ erg s $^{-1}$ cm $^{-2}$). MAXI observes very nearly the full sky each ~ 90 minute orbit. We adopt this fluence as a detection threshold. (Because the prompt emission is short compared to the exposure timescale, fluence and not flux is the critical quantity.) In calculating the X-ray emission, we arbitrarily assume that a fraction $f_X = 10\%$ of the impact energy E is released in the form of prompt (nonthermal) X-rays.

By contrast, Chandra / XMM-Newton imaging is sensitive to *much* fainter X-ray sources. The tradeoff, of course, is that these instruments have very narrow fields-of-view, and a correspondingly low duty cycle for observing any particular region of sky. We neglect photon pileup effects, and adopt a detection threshold of 25 X-ray photons (at a characteristic energy of 1 keV, for an instrument with effective area ~ 300 cm 2).

In Table 1, we compute rough estimates for the rate, brightness, and detectability of impact events across a spectrum of masses. The impactor masses we consider range from 10^{14} g, based on a lower optical threshold of $\tilde{L}_{\text{opt}} = 10^{29}$ erg/s, to Jupiter’s mass, 10^{30} g. In each case, we give the maximum distance for which the event could be detected in the optical and X-ray detectors discussed above.

Asteroids of mass $\lesssim 10^{20}$ g produce the least energetic events in Table 1. These are most readily detected in the optical, just within our Galaxy (or even just the Solar neighborhood). Although event rates are high, so that hundreds to thousands of events are

Table 1. Event Rate and Detectability

Mass (g)	Rate ($\text{yr}^{-1} \text{Galaxy}^{-1}$)	Peak \bar{L}_{opt} (erg/s)	$f_X E/1\text{keV}$ photons	d_{opt} (pc)	$d_{X,\text{imag}}$ (pc)	$d_{X,\text{monitor}}$ (pc)	Best Strategy
10^{14} (103P/Hartley 2)	8×10^6	10^{29}	10^{39}	150	8	0.08	Ground-based optical surveys.
10^{17} (SL9)	4×10^4	10^{32}	10^{42}	5×10^3	250	2.5	Ground-based optical surveys.
10^{19} (Eros)	10^3	10^{34}	10^{44}	50×10^3	2.5×10^3	25	Ground-based optical surveys.
10^{22} (Iris)	8	10^{37}	10^{47}	1500×10^3	80×10^3	800	X-ray all-sky monitors.
10^{24} (Ceres)	0.25	10^{39}	10^{49}	15×10^6	800×10^3	8×10^3	X-ray all-sky monitors.
10^{26} (Mercury)	0.008	10^{41}	10^{51}	150×10^6	8×10^6	80×10^3	X-ray imaging of galaxy clusters.
10^{28} (Earth)	2.5×10^{-4}	3×10^{42}	10^{53}	800×10^6	80×10^6	800×10^3	X-ray imaging of galaxy clusters.
10^{30} (Jupiter)	8×10^{-6}	2×10^{44}	10^{55}	7×10^9	800×10^6	8×10^6	X-ray imaging / all-sky monitors.

Note. — Estimates are subject to an approximate ~ 1 order of magnitude uncertainty.

detectably bright, these transient impacts are so brief that even high-cadence ground-based surveys designed to hunt transients are only likely to find 0.1–1 per decade (being most sensitive to impactors with $M \sim 10^{19}\text{g}$).

Meanwhile, energetic events involving sub-Earth-mass planets ($M \sim 10^{27}\text{g}$) occur with sufficient frequency that they are potentially detectable with X-ray imaging of galaxy clusters. In particular, several Ms aggregate imaging is available for crowded fields of nearby rich clusters ($d \lesssim 100$ Mpc, e.g., Virgo, Norma, and Coma). Our model predicts $\lesssim 0.1$ events in the aggregate data set. However, we speculate that the vigorous dynamical activity in clusters may enhance these rates.

Intermediate impactor masses just below the scale of Ceres ($M \lesssim 10^{24} \text{ g}$), are sufficiently faint that they are all but undetectable outside the Local Group. At the same time, the collision rates are so low that pointed ground or space-based instruments have negligible chance at serendipitous discovery. In this regime, the X-ray monitors shine. Nearly 1 event per year is detectably bright by an X-ray monitor; however, factoring in the sky coverage, only 0.01 – 0.1/yr detections are expected.

Next decade, LSST, with its tenfold improvement in sensitivity is well-poised to make dozens of detections of events by both the lowest-mass and highest-mass mass impactors. In particular, we predict that tens of Galactic events involving impactors with $M = (10^{14} - 10^{18}) \text{ g}$ will be detected in the first year. The dominant sensitivity is for masses $M \sim 10^{16} \text{ g}$, which roughly corresponds to the lowest-mass impactor for which the detectable volume is matched to the scale of the Galaxy. We predict tens of planet impact detections each year: we expect an annual rate of roughly one Mercury-scale detection, and nearly ten Jupiter-mass event detections. In the latter instance, the signal is dominated by high redshift events ($z \approx 1 - 3$).

In short, we find that with current instruments, WD-planetesimal impacts are at

the cusp of detectability. It is unlikely that any event has heretofore been identified or recorded. At the same time, we note that with a generational improvement in sensitivity for X-ray coded-mask instruments, or in the forthcoming LSST at optical wavelengths, we will be well-poised to discover such impact events. Notably, a modest improvement in X-ray monitor sensitivity would critically extend the detectability of Jupiter-WD collisions out to distances of $\gtrsim 100$ Mpc, the proximity of nearby galaxy clusters. Detection rates for these most energetic events would then become appreciable. Even as we wait for a statistical sample of these events to be established using the rich capabilities of LSST, in this decade monitoring programs by PTF, Pan-STARRS, and other campaigns such as OGLE will be increasingly capable of discovering a nearby planetoid-WD impact.

3. The Progenitors of Type Ia Supernovae

3.1. Possibilities and Caveats

WD-planetoid collisions are frequent enough that if only one in $\sim 10^7 - 10^8$ produces an SN Ia, death-by-dynamics models will contribute significantly to the total rate. To trigger an SN Ia, a collision must dynamically ignite matter on a WD's surface. This requires compressing and heating material above a critical temperature where the burning time becomes comparable to the dynamical time. For pure hydrogen, the critical mass to auto-ignite a thin atmosphere is small, and such WDs have very little in their atmospheres (no more than $10^{-4} M_{\odot}$). For pure helium, the maximum envelope mass can be tenths of a solar mass for low-mass WDs ($\sim 0.5M_{\odot}$), and decreases with increasing accretor mass ([Bildsten et al. 2007](#)).

If, however, a part of the envelope is compressed and/or heated above its steady-state condition, the fluid can spawn a self-supporting nuclear detonation that propagates

throughout the envelope. Initiating such a detonation involves heating a mass far smaller than the total envelope mass. For pure helium, this mass is on the order of Earth’s mass. Hence, we would expect that, at minimum, the total impacting mass required to initiate a detonation in the helium layer should be equal to this value. Furthermore, the conditions for detonation are usually realized at the interface between the outer envelope and the inner core. In cases where the outer envelope mass is large, an impactor would need to penetrate through a mass greater than its own to reach the depth of this interface. Secondly, planetary/planetesimal impactors are low-density, an Earth-mass body has roughly the same size as the WD, and its kinetic energy is spread over a large shell (meanwhile, the critical length scales are derived presuming all the mass lies within a small, spherical volume).

We envision two circumstances which could change this picture. Firstly, the critical length scales have only been calculated for a few composition combinations, namely carbon-oxygen ([Seitenzahl et al. 2009](#)), and pure helium ([Holcomb et al. 2013](#)). However, the inclusion of even a small admixture of heavy nuclei into a helium layer will greatly reduce the burning timescale, since α captures onto these nuclei are far more rapid than the relatively slow $3\text{-}\alpha$ reaction ([Shen & Moore 2014](#)). Consequently, while a single impact may not detonate a pure helium envelope, repeated bombardment may contaminate the envelope to such a degree that α captures and other nuclear pathways become viable. Secondly, because the impact is fundamentally a dynamical process, the geometry of the impact may lead to a shock-focused detonation in a layer stable to a single hot spot generated by the collision – see e.g., [Fink et al. \(2010\)](#).

3.2. Death by Dynamics in Tandem with SD and DD models

The two leading models for SN Ia progenitors invoke interacting binaries with epochs of mass transfer and common envelope evolution. These epochs last long enough to permit sequences of planetoid interactions. In single degenerate (SD) models, a non-degenerate companion donates matter to the WD. In double degenerate (DD) models two WDs merge, leading to a detonation.

Planetoid interactions that enrich the WD may alter SN Ia rates in three ways. Firstly, if enrichment extends (narrows) the range of infall rates compatible with steady nuclear burning (Piersanti et al. 2014), then both DD and SD rates would be affected. Secondly, enhanced metallicity increases winds, possibly stabilizing mass transfer for systems verging on dynamical instability. Finally, enrichment may make it easier or harder to spark explosions during the accretion/merger processes associated with explosions in SD/DD models. Furthermore, a subset of planetoid interactions with the donor, disk, or common envelope could alter the binary’s further evolution.

3.3. Predictions of Death-by-dynamics Models

Death-by-dynamics models predict diversity among SNe Ia. The WD mass does not have a fixed value at explosion. Differences in planetoid compositions produce chemical diversity. These models are novel in positing that a WD can become an SN Ia without a close companion. There may, however, be other stars near the WD: distant bound companions, passing stars which have triggered planetoid interactions, or even close interacting companions. Thus, the properties of any stars in the field close to the SN may exhibit a variety of luminosities and spectral types. The circumstellar region may be enriched with planetary debris that interacts with the supernova.

Early-time explosions are predicted by death-by-dynamics models, because stellar evolution destabilizes planetoid orbits. As well, planetoids continue to be placed on eccentric orbits over a Hubble time. The combination of strong early-time signals and continuation through late times is consistent with data on SNe Ia (e.g., [Sullivan et al. \(2006\)](#)). Calculations are needed to check whether the distribution of death-by-dynamics delay times is consistent with observations.

The discovery of WD-planetoid collision events will identify environments that produce SNe Ia through death-by-dynamics channels. Conversely, regions producing SNe Ia must be rich in WD-planetoid interactions.

4. Conclusions

WD-planetoid collisions produce bright, detectable events. Observing these events will measure peak luminosities and time evolution in broad energy bands, and will quantify environmental effects. This will provide clues to the mass distributions of both planetoids and WDs, and eventually chemical information. Such studies are possible because large numbers of planetoids orbit WDs and large numbers of WDs inhabit galaxies. Even unusual interactions and sequences of interactions are common in galaxies and galaxy clusters.

A planetoid interaction or sequence of them may spark SNe Ia. The exploding WDs may be isolated or may be in interacting binaries. While it will be challenging to test death-by-dynamics SNe Ia progenitor models, we note that this has also been true for SD and DD models. Fortunately, if death-by-dynamics models do produce SNe Ia, they make a host of predictions, some of which can be tested through the study of bright events caused by WD-planetoid collisions. In summary, death-by-dynamics models make testable predictions and suggest intriguing directions for future investigations.

Acknowledgements: RD thanks Stuart Sim and Rüdiger Pakmor for enlightening discussions. This work was supported by NSF AST-1211843, AST-0708924, AST-0908878 and NASA NNX12AE39G, AR-13243.01-A. JFS was supported by the NASA Hubble Fellowship HST-HF-51315.01. JG was supported by the NASA Einstein Fellowship PF3-140108.

REFERENCES

- Arnett, W. D. 1980, *ApJ*, 237, 541
- Asphaug, E., & Benz, W. 1996, *Icarus*, 121, 225
- Barber, S. D., Patterson, A. J., Kilic, M., Leggett, S. K., Dufour, P., Bloom, J. S., & Starr, D. L. 2012, *ApJ*, 760, 26
- Barthelmy, S. D., et al. 2005, *Space Sci. Rev.*, 120, 143
- Bildsten, L., Shen, K. J., Weinberg, N. N., & Nelemans, G. 2007, *ApJ*, 662, L95
- Di Stefano, R. 2011, *Planets Orbiting White Dwarfs*, ed. D. W. Hoard, 89–116
- Djorgovski, S. G., et al. 2008, *Astronomische Nachrichten*, 329, 263
- Drake, A. J., et al. 2009, *ApJ*, 696, 870
- Farihi, J., Gänsicke, B. T., & Koester, D. 2013, *Science*, 342, 218
- Fink, M., Röpke, F. K., Hillebrandt, W., Seitenzahl, I. R., Sim, S. A., & Kromer, M. 2010, *A&A*, 514, A53
- Fryxell, B., et al. 2000, *ApJS*, 131, 273
- Fuentes, C. I., Holman, M. J., Trilling, D. E., & Protopapas, P. 2010, *ApJ*, 722, 1290
- Holcomb, C., Guillochon, J., De Colle, F., & Ramirez-Ruiz, E. 2013, *ApJ*, 771, 14
- Jura, M. 2008, *AJ*, 135, 1785
- Kaiser, N., et al. 2002, in *Society of Photo-Optical Instrumentation Engineers (SPIE) Conference Series*, Vol. 4836, *Survey and Other Telescope Technologies and Discoveries*, ed. J. A. Tyson & S. Wolff, 154–164

- Keller, S. C., et al. 2007, *PASA*, 24, 1
- Koester, D. 2009, *Astronomy & Astrophysics*, 498, 517
- Levine, A. M., Bradt, H., Cui, W., Jernigan, J. G., Morgan, E. H., Remillard, R., Shirey, R. E., & Smith, D. A. 1996, *ApJ*, 469, L33
- Mihara, T., et al. 2011, *PASJ*, 63, 623
- Nelemans, G., Toonen, S., & Bours, M. 2013, in *IAU Symposium*, Vol. 281, *IAU Symposium*, ed. R. Di Stefano, M. Orío, & M. Moe, 225–231
- Parriott, J., & Alcock, C. 1998, *Astrophysical Journal* v.501, 501, 357
- Perryman, M. A. C., et al. 2001, *A&A*, 369, 339
- Piersanti, L., Tornambé, A., & Yungelson, L. R. 2014, *MNRAS*, 445, 3239
- Pineault, S., & Landry, S. 1994, *MNRAS*, 267, 557
- Rau, A., et al. 2009, *PASP*, 121, 1334
- Schlichting, H. E., Fuentes, C. I., & Trilling, D. E. 2013, *AJ*, 146, 36
- Seitzzahl, I. R., Meakin, C. A., Townsley, D. M., Lamb, D. Q., & Truran, J. W. 2009, *ApJ*, 696, 515
- Shen, K. J., & Moore, K. 2014, *ApJ*, 797, 46
- Sullivan, M., et al. 2006, *ApJ*, 648, 868
- Ubertini, P., et al. 2003, *A&A*, 411, L131
- Zuckerman, B., Melis, C., Klein, B., Koester, D., & Jura, M. 2010, *ApJ*, 722, 725